Journal of Petroleum Science and Engineering 164 (2018) 400–416

Contents lists available at ScienceDirect

Journal of Petroleum Science and Engineering

journal homepage: www.elsevier.com/locate/petrol

A stability-improved efficient deconvolution algorithm based on B-splines by appending a nonlinear regularization

Wenchao Liu [a,b,*], Yuewu Liu [b], Weiyao Zhu [a], Hedong Sun [c]

[a] School of Civil and Resource Engineering, University of Science and Technology Beijing, Beijing 100083, PR China
[b] Institute of Mechanics, Chinese Academy of Sciences, Beijing 100190, PR China
[c] Department of Gas Field Development, PetroChina Research Institute of Petroleum Exploration and Development, Langfang, Hebei 065007, PR China

ARTICLE INFO

Keywords:
Deconvolution
Nonlinear least-squares problem
Duhamel principle
Stability improvement
Second-order B-spline functions

ABSTRACT

Previous deconvolution algorithms based on B-splines are much easier to be understood and programmed for academic researchers and engineers. However, due to the use of a linear regularization, their stability is weaker than that of the commonly used von Schroeter et al.'s deconvolution algorithm in which a nonlinear regularization is used; the linear regularization can make the deconvolution algorithms less tolerant to data errors. Good stability for the deconvolution algorithms is very important in order to make deconvolution as a viable tool for well-test analysis. In the paper, in order to improve the stability of the deconvolution algorithms based on B-splines, a nonlinear regularization by minimizing the curvature of pressure derivative response, as used in von Schroeter et al.'s algorithm, is appended instead of the linear regularization. And the corresponding nonlinear regularization equations are appropriately deduced. In particular, the improved algorithm is based on the Duhamel principle directly, and the complex transformation by the nonlinear z function, as used in von Schroeter et al.'s algorithm, is avoided; it does simplify the whole deconvolution process; moreover, the sensitivity matrix of an involved basic linear system from the measured pressure and rate data can also be solved directly by the piecewise analytical integration method, which can largely improve the deconvolution computation speed. Ultimately, in combination with the nonlinear regularization equations, a nonlinear least-squares problem is formulated for the stability-improved deconvolution algorithm based on B-splines. Besides, a constraint condition for tuning the parameter values of the B-spline base and an involved smooth factor is presented for restricting the nonlinear regularization process. Through a simulated case study, it is found that the nonlinear least-squares problem can be solved stably by the advanced Powell's Dog Leg method due to its great convergence ability and numerical stability; and the solution accuracy is also verified. Then the effects of the two parameters on the type curves of the deconvolution results are analyzed. And the effect of the error in the initial formation pressure on the type curves of the deconvolution results is also analyzed. Then a statement on how to perform the nonlinear regularization is presented specifically.

Furthermore, through the study on two simulated cases with added data errors and an actual case, it is demonstrated that when the nonlinear regularization is appended, the stability of the deconvolution algorithm based on B-splines can be largely improved for mitigating the effect of data errors; besides, the stability-improved algorithm based on B-splines even exhibits higher stability than von Schroeter et al.'s algorithm that takes the same nonlinear regularization method, and the reason can be attributed to the superior properties of the representation of the wellbore pressure derivative (to be deconvolved) by B-spline functions in the numerical stability of computations and the inherent smoothness. Through the test of some simulated cases, it is also concluded that the stability-improved algorithm based on B-splines by appending the nonlinear regularization still has a high-level computation speed, which is nearly twenty times more than that of von Schroeter et al.'s algorithm. It can be attributed to the more undetermined coefficients and the computational complexity resulted from the z-function transformation in the formulation of von Schroeter et al.'s algorithm.

* Corresponding author. School of Civil and Resource Engineering, University of Science and Technology Beijing, Beijing 100083, PR China.
E-mail address: wcliu_2008@126.com (W. Liu).

https://doi.org/10.1016/j.petrol.2018.01.083
Received 19 August 2017; Received in revised form 9 December 2017; Accepted 31 January 2018
Available online 5 February 2018

1. Introduction

The deconvolution based on Duhamel principle has been widely applied in the well testing technology in reservoir engineering. The inverse problem can provide the equivalent constant unit production rate pressure response of the well in a reservoir system that is affected by the variable production rates for the entire duration of the production history. The relevant deconvolution algorithms have attracted big attentions over the past forty years (Liu et al., 2017). Due to the commonly existent errors of wellbore pressure and production rate data in the fields, the deconvolution computation is always ill-conditioned inherently (Çınar et al., 2006). As far as we know, although many deconvolution algorithms have been proposed, just several ones appear to exhibit the stability of data error tolerance; they are proposed by von Schroeter et al. (von Schroeter et al., 2002; von Schroeter et al., 2004), Levitan et al. (Levitan, 2005; Levitan et al., 2006) and Ilk et al. (Ilk, 2005; Ilk et al., 2005; Liu et al., 2017), respectively. Here, these aforementioned different deconvolution algorithms will be introduced in details. In addition, it is worth to mention that recently Ahmadi et al. (2017) present a new robust deconvolution algorithm with the minimum user interference, which combines the conveniences of deconvolution in Laplace domain with a new approach to transform the sampled data from time domain to Laplace domain without extrapolating the data beyond the sampling interval; Ahmadi et al.'s algorithm overcomes the limitations of the requirement that the piecewise functions for the sampled data representation should be defined in the complex plane for the application of deconvolution in Laplace domain (Al-Ajmi et al., 2008).

It is well known that the Duhamel principle (Çınar et al., 2006) is as follows:

$$p_{\mathrm{ini}} - p = \int_0^t q(t-\tau)p_{\mathrm{u}}^{'}(\tau)\mathrm{d}\tau \tag{1}$$

where t is the time; τ is a variable for the integral; q is the measured variable rate; p is the measured wellbore pressure corresponding to the variable rate; p_{u} is the wellbore pressure drop corresponding to the constant unit rate; p_{ini} is the initial formation pressure. The aim of these deconvolution algorithms is to obtain p_{u} when the data of q and p are both given.

In order to make sure the positivity of $\mathrm{d}p_{\mathrm{u}}/\mathrm{dln}(t)$ for the relevant plotting of type curves, z function is defined in von Schroeter et al.'s deconvolution algorithm (von Schroeter et al., 2002; von Schroeter et al., 2004), as follows:

$$z = \ln\left[\frac{\mathrm{d}p_{\mathrm{u}}(t)}{\mathrm{dln}(t)}\right] \tag{2}$$

Then Eq. (1) can be equivalently transformed as follows:

$$p_{\mathrm{ini}} - p = \int_{-\infty}^{\ln t} q(t-\mathrm{e}^{\tau})\mathrm{e}^{z(\tau)}\mathrm{d}\tau \tag{3}$$

Then the aim turns to the solution of z. von Schroeter et al.'s deconvolution algorithm (von Schroeter et al., 2002; von Schroeter et al., 2004) accounts for the fitting errors for both the measured pressure data and rate data; in order to improve the smoothness of the solution of z when data errors exist, minimization of the curvature of z function is appended as a nonlinear regularization method. As a result, a total nonlinear least-squares problem is formulated. As for Levitan et al.'s deconvolution algorithm (Levitan, 2005; Levitan et al., 2006), their ideas are also from von Schroeter et al.'s deconvolution algorithm. They are both based on the same concept of minimizing a nonlinear weighted least-square objective function, involving the sum of three mismatch terms including the pressure, the rate and the curvature, for reconstructing the deconvolved pressure drop and its logarithmic derivative (Liu et al., 2017). The difference of the two algorithms mainly lies in the aspects of model assumption and the specific definition of objective functions. Due to the use of nonlinear regularization i. e. the minimization of the curvature instead of the pressure derivative (Ilk, 2005; Ilk et al., 2005), von Schroeter et al.'s deconvolution algorithm can exhibit relatively higher stability when data errors exist (Çınar et al., 2006).

Another different deconvolution algorithm based on B-splines is proposed by Ilk et al. first (Ilk, 2005; Ilk et al., 2005). The algorithm is based on Eq. (1) directly, and the transformation of Eq. (1) by the nonlinear z function is avoided; a weighted summation of second-order B-splines is adopted to reconstruct $p_{\mathrm{u}}^{'}$; and a linear regularization method is adopted to overcome the effect of data errors, which can make the logarithmic derivative of p_{u} differ slightly between the B-spline knot and the middle location between knots (Ilk, 2005; Ilk et al., 2005). In combination with Laplace transform and numerical Laplace inversion, the formulated linear least-squares problem can be solved. What's more, Ilk et al.'s algorithm is further improved by Liu et al. (2017) through a technique of piecewise analytical integration for calculating the involved sensitivity matrix (Liu et al., 2017) in the real time space instead of the Laplace space; then the success of the deconvolution computation based on B-splines can be guaranteed, and the improved deconvolution algorithm exhibits big advantage in the fast computational speed due to the use of the analytical solution method.

Good stability of deconvolution algorithms is very necessary in order to make deconvolution as a viable tool for well-test analysis; and stability improvement is also the main difficulty in the development of deconvolution algorithms. Çınar et al. (2006) have ever conducted a comparative study on these deconvolution algorithms mentioned above: Significantly, it is found that the weaker linear regularization method applied in the deconvolution algorithms based on B-splines (including Ilk et al.'s deconvolution algorithm (Ilk, 2005; Ilk et al., 2005) and its improved version by Liu et al. (2017)) can make the algorithms less tolerant to data errors; in contrast, von Schroeter et al.'s deconvolution algorithm shows relatively higher stability by using the nonlinear regularization method, and the deconvolution algorithm has been implemented into Saphir as the pressure transient analysis module of KAPPA software due to its good stability. However, in von Schroeter et al.'s deconvolution algorithm, the transformed deconvolution equation of Duhamel principle i. e. Eq. (3) is used, which makes the computation process become very complicated; in contrast, the deconvolution equation of Duhamel principle i. e. Eq. (1) is directly used in the algorithms based on the B-splines, and the involved sensitivity matrix can also be solved directly by the piecewise analytical integration method, which can largely improve the computation speed; and its computation procedures are much easier to be understood and programmed for academic researchers and engineers. What's more, representation of the unknown function by B-spline functions, which are piecewise defined polynomial functions, has superior properties such as local effects of coefficients, numerical stability of computations and inherent smoothness (Jauch et al., 2017) in comparison with representation of the unknown function by piecewise linear approximations as used in von Schroeter et al.'s algorithm. Therefore, in view of the above-mentioned facts, it is very necessary to further improve the stability of the algorithms based on B-splines. For the purpose, an idea can be presented naturally that the nonlinear regularization method in von Schroeter et al.'s algorithm may be applied into the algorithms based on B-splines.

In this paper, based on the improved version of Ilk et al.'s deconvolution algorithm (Liu et al., 2017), the nonlinear regularization method, as used in von Schroeter et al.'s deconvolution algorithm, is appended so as to largely improve the stability of the algorithms based on B-splines. It can make the deconvolution algorithm based on B-splines to be more acceptable and more advanced for its applications in the well testing technology. The schematics for the stability improvement of the deconvolution algorithm based on B-splines are shown in Fig. 1. From Fig. 1, it can be seen that the stability-improved algorithm can inherit good "genes" including the representation of $p_{\mathrm{u}}^{'}$ by B-splines (Liu et al., 2017), no complicated z-function transformation of the convolution equation (Liu et al., 2017), the fast analytical solution method for calculating the elements of sensitivity matrix (Liu et al., 2017) and the nonlinear

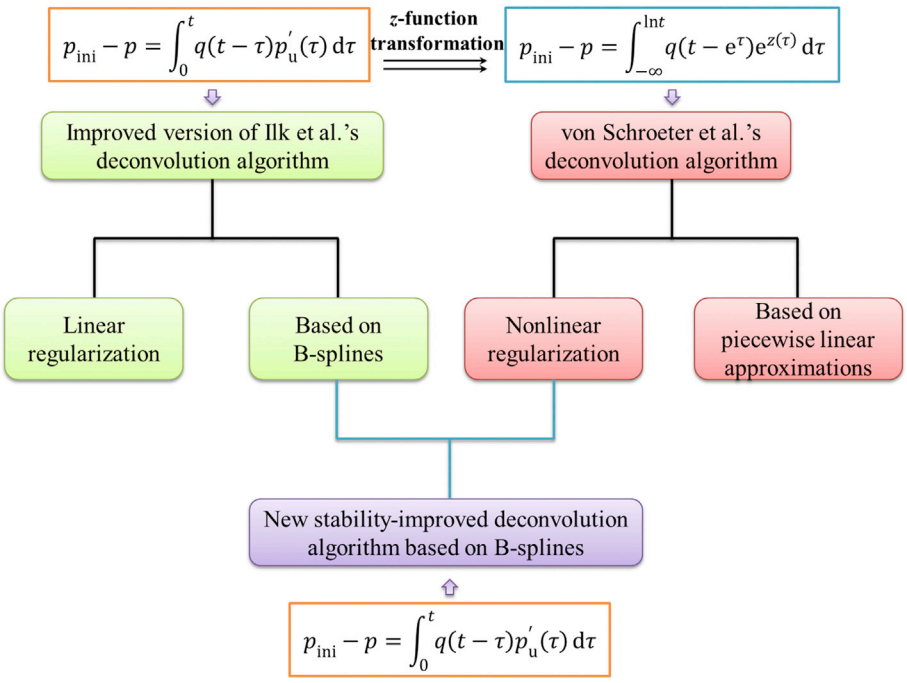

Fig. 1. The schematics for the stability improvement of the deconvolution algorithm based on B-splines.

regularization method (von Schroeter et al., 2002; von Schroeter et al., 2004) from their "parents": The improved version of Ilk et al.'s deconvolution algorithm based on B-splines (Liu et al., 2017) and von Schroeter et al.'s deconvolution algorithm (von Schroeter et al., 2002; von Schroeter et al., 2004).

2. Stability improvement of deconvolution algorithms based on B-splines

2.1. Generation of the basic linear system from the measured pressure and rate data

According to the Ilk et al.'s algorithm based on B-splines, p_u' is represented by a weighted summation of second-order B-splines (Ilk, 2005; Ilk et al., 2005), as follows:

$$p_u'(t) = \sum_{i=1}^{w} c_i B_i^2(t) \tag{4}$$

where c_i is the undetermined weight coefficient; w is the number of undetermined coefficients; $B_i^2(t)$ is the second-order B-spline (Ilk, 2005; Ilk et al., 2005). In order to make the log-log curves of the deconvolved p_u' more smooth, it is required reasonably that the knots should be distributed logarithmically as b^l ($l = 0, \pm1, \pm2, \ldots$) for the generation of second-order B-splines; please refer to the literatures (Ilk, 2005; Ilk et al., 2005) for the details of the B-spline generation process; and the distribution range of the knots must cover the time range of these measured pressure data. The selection of the base b for the generation of second-order B-splines should also satisfy the condition that the number of knots per log cycle is on the order of at least 2–6 knots (Ilk, 2005; Ilk et al., 2005).

Then substituting Eq. (4) into the Duhamel principle i. e. Eq. (1) directly yields:

$$p_{ini} - p(t) = \sum_{i=1}^{w} c_i \int_0^t q(\tau) B_i^2(t-\tau)\,d\tau \tag{5}$$

It is assumed that the total number of the measured wellbore pressure p data is N_p; and the measured variable production rate q data and the initial formation pressure p_{ini} are known. Then by substituting the measured pressure and variable rate data into Eq. (1), a linear system with respect to c_i can be obtained, as follows:

$$\mathbf{XC} = \mathbf{\Delta P} \tag{6}$$

where $\mathbf{X}$ is the $N_p \times w$ sensitivity matrix; $\mathbf{C}$ is the w-vector of undetermined coefficients c_i; and $\mathbf{\Delta P}$ is the N_p-vector of measured wellbore pressure drop.

According to Eq. (5), the calculation of the elements of the sensitivity matrix $\mathbf{X}$ needs to solve the corresponding convolution integrals (Liu et al., 2017). Solution by the numerical integration method is time-consuming. As the z-function transformation (von Schroeter et al., 2002; von Schroeter et al., 2004) is not taken, in order to largely improve the deconvolution computation speed, the elements of the sensitivity matrix $\mathbf{X}$ can be fast solved analytically by the technique of piecewise analytical integration method according to the real production rate history (Liu et al., 2017); please refer to the reference (Liu et al., 2017) for the details.

In addition, it is worth to point out that although the z-function transformation i. e. Eq. (2) is avoided in the new stability-improved algorithm, the deconvolved $dp_u/d\ln(t)$ can still keep positive for the plotting of type curves, which will be shown in all the following case study in the paper.

2.2. Generation of a nonlinear system from the nonlinear regularization

In Ilk et al.'s algorithm, a weak linear regularization method is used for ensuring the relevance of the spline representation with the type curves from reservoir modeling (Ilk, 2005; Ilk et al., 2005; Liu et al., 2017). Here, in order to further improve the stability, a nonlinear regularization (von Schroeter et al., 2002; von Schroeter et al., 2004) by minimizing the curvature of pressure derivative response, which has been used in von Schroeter et al.'s deconvolution algorithm, is appended in the new algorithm based on B-splines instead of the linear regularization in the original Ilk et al.'s algorithm (Ilk, 2005; Ilk et al., 2005; Liu et al., 2017). And the relevant equation for the nonlinear regularization is also deduced based on the representation of p_u' by B-splines.

Three points of pressure derivative response at three successive knots

of B-splines at log-log coordinates are shown in Fig. 2. The three successive knots are t_{s-1}, t_s and t_{s+1}, respectively. Correspondingly, the coordinate of the three points of pressure derivative p'_u in the log-log coordinate system are A point: $(\log(t_{s-1}), \log(t_{s-1}\cdot p'_u(t_{s-1})), 0)$, B point: $(\log(t_s), \log(t_s\cdot p'_u(t_s)), 0)$ and C point: $(\log(t_{s+1}), \log(t_{s+1}\cdot p'_u(t_{s+1})), 0)$. The added coordinate component zero for every point is for the upcoming multiplication cross of vectors. Due to the reality that a large amount of information is from the slopes of the graphed p'_u, the accurate description of the smoothness should be in terms of curvature of the graph instead of penalizing derivatives (von Schroeter et al., 2002; von Schroeter et al., 2004). In Fig. 2, the angle between the vector $\overrightarrow{AB}$ and the vector $\overrightarrow{BC}$ is written as θ_s, which can represent the curvature of the type curve (von Schroeter et al., 2002; von Schroeter et al., 2004). In order to make the type curve smooth, θ_s is set as zero. Equivalently, the sine of θ_s is set as zero. $\sin(\theta_s)$ can be calculated through the multiplication cross of the vector $\overrightarrow{AB}$ and the vector $\overrightarrow{BC}$, as follows:

$$|\sin(\theta_s)| = \left|\frac{\overrightarrow{AB}\times\overrightarrow{BC}}{|\overrightarrow{AB}|\cdot|\overrightarrow{BC}|}\right| = 0 \tag{7}$$

Eq. (7) is equivalent to the following equation:

$$\overrightarrow{AB}\times\overrightarrow{BC} = 0 \tag{8}$$

From Eq. (8), the nonlinear regularization equations can be deduced as follows:

$$\beta\cdot\log\left(\frac{t_s}{t_{s-1}}\right)\cdot\log\left(\frac{t_{s+1}\cdot p'_u(t_{s+1})}{t_s\cdot p'_u(t_s)}\right) - \beta\cdot\log\left(\frac{t_{s+1}}{t_s}\right)\cdot\log\left(\frac{t_s\cdot p'_u(t_s)}{t_{s-1}\cdot p'_u(t_{s-1})}\right) = 0 \tag{9}$$

where β is the smooth factor as the weight for the nonlinear regularization.

In order to make the values of the antilog of the logarithmic functions in Eq. (9) positive in the involved computational solution process by iterations, the equation is rewritten equivalently, as follows:

$$\beta\cdot\log\left(\frac{t_s}{t_{s-1}}\right)\cdot\log\left(\left(\frac{t_{s+1}\cdot p'_u(t_{s+1})}{t_s\cdot p'_u(t_s)}\right)^2\right) - \beta\cdot\log\left(\frac{t_{s+1}}{t_s}\right)\cdot\log\left(\left(\frac{t_s\cdot p'_u(t_s)}{t_{s-1}\cdot p'_u(t_{s-1})}\right)^2\right) = 0 \tag{10}$$

It should be noted that in order to avoid the emergence of zero values of p'_u at the initial and final knots of B-splines, the range of index s of knot t_s is set from 2 to K_P-2; K_P is the total number of the knots.

In the well testing, it is known that the initial period is the wellbore storage period, and the unit slope of pressure derivative of the type curve commonly exists at the log-log coordinates. Therefore, the first vector can be expressed as (1, 1, 0). Then when $s = 2$, the first nonlinear regularization equation can be simplified as follows:

$$\beta\cdot\log\left(\left(\frac{t_3\cdot p'_u(t_3)}{t_2\cdot p'_u(t_2)}\right)^2\right) - \beta\cdot\log\left(\left(\frac{t_3}{t_2}\right)^2\right) = 0 \tag{11}$$

2.3. A combined nonlinear system as a nonlinear least-squares problem

As the nonlinear regularization is appended with the weight β, the basic linear system generated i. e. Eq. (6) from the measured pressure and rate data should be further expressed equivalently, as follows:

$$(1-\beta)\cdot\mathbf{XC} = (1-\beta)\cdot\Delta\mathbf{P} \tag{12}$$

where $0 \le \beta < 1$.

As a result, Eqs. (10–12) together form an overdetermined nonlinear system i. e. a nonlinear least-squares problem for the stability-improved deconvolution algorithm based on B-splines. The aim is to obtain **C** by solving the nonlinear least-squares problem.

For numerically solving the nonlinear problem, the common Gauss-Newton method may not converge if the guessed iteration starting point is far from the global minimum. Therefore, in order to overcome the problem, as Madsen et al. suggested (Madsen et al., 2004), two advanced methods including the Levenberg-Marquardt method and the Powell's Dog Leg method are selected for the solution testing. They are both a combination of the Gauss-Newton method and the steepest descent method: When the approximated solution is far from the global minimum, the steepest descent step is taken; and when the approximated solution is very close to the global minimum, Gauss-Newton step is taken (Shterenlikht and Alexander, 2012). In particular, for the Powell's Dog Leg method, the radius of a trust region is used for explicitly controlling the step directions. The two methods have much higher stability than the Gauss-Newton method (Madsen et al., 2004).

2.4. A constraint for tuning deconvolution parameters

When **C** is calculated, the reconstructed pressure response $p(t)$ by B-splines i. e. the back-calculated pressure response $p(t)$ from Eq. (5) can be compared with the measured wellbore pressure data. It can be used as a direct constraint condition (Liu et al., 2017) for tuning the value assignment of the base b of B-splines and the smooth factor β during the nonlinear regularization process. The detailed statement on how to perform the regularization will be illustrated in the following case study.

2.5. Application conditions for the deconvolution algorithm

The stability-improved deconvolution algorithm is only applicable for a linear system, due to the reason that the Duhamel principle i. e. Eq. (1) only holds in the linear system. The deconvolution algorithm should be applied to only the consistent measured wellbore pressure and production rate data with high quality. In practice, the nonlinearity (inconsistency) may come from some reservoir behaviors such as the variable skin factor, the variable wellbore storage coefficient, the multiphase flow, the changing reservoir permeability, the commingled production from different layers and the inter-well interference effect; the algorithm can't be used for the deconvolution of the data at any well test periods after the nonlinear phenomena occur (Onur et al., 2008; Onur and Kuchuk, 2012). However, as discussed by Onur and Kuchuk (2012), if the nonlinearity is weak, the deconvolution may be still applicable.

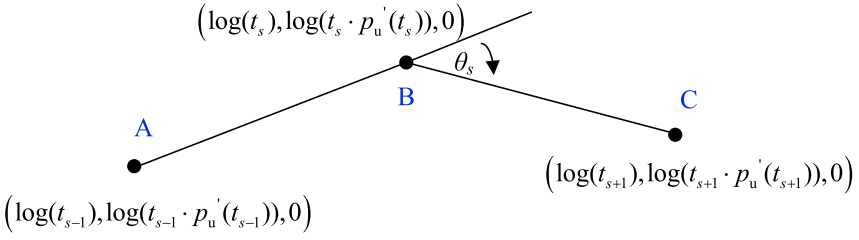

Fig. 2. The schematics of three successive pressure derivative points at log-log coordinates.

It has been well known that the deconvolution algorithm is very sensitive to the small error in the initial formation pressure (Levitan et al., 2006; Onur et al., 2008; Onur and Kuchuk, 2012; Ahmadi et al., 2017). As discussed by Levitan (2006), the initial formation pressure should be known in the deconvolution. The effect of the error in the initial formation pressure on the deconvolution results will be analyzed in the Section 3.3. In addition, the production rate data should be accurate sufficiently in order to obtain accurate results by the deconvolution algorithm (Onur and Kuchuk, 2012).

3. Algorithm testing through simulated case study

3.1. Accuracy verification of the stability-improved deconvolution algorithm

The simulated case is a problem of radial single-phase Darcy's flow into a vertical production wellbore in an infinite dual-porosity reservoir; the reservoir is homogeneous, isotropic and isothermal; the horizontal flow does not have any gravity effect. The Newtonian fluid and rocks are both slightly compressible. The values of the reservoir parameters are shown in Table 1. The production history for the production well includes eight production durations, and the specific production rate data is listed in Table 2.

The simulated wellbore pressure data corresponding to the variable production rate data through the KAPPA software is shown in Fig. 3. The total number of the wellbore pressure data is 426. The initial reservoir pressure is 30.0 MPa. The wellbore pressure response corresponding to the unit production rate 1.0 STB/D for the whole production duration i. e. 400 days is also obtained through the simulation by the KAPPA software, which is shown in Fig. 4.

The stability-improved deconvolution algorithm is performed to transfer the wellbore pressure data corresponding to the variable production rate in Fig. 3 into the one corresponding to the unit production rate 1.0 STB/D. The Levenberg-Marquardt method and the Powell's Dog Leg method are both tested for solving the resulted nonlinear least-squares problem for the simulated case in Fig. 3; it is worth to mention that the search for $\{c_i,\ i = 1, \ldots, w\}$ by iterations by the two methods both starts from $\{c_i = c_0,\ i = 1, \ldots, w\}$, where c_0 is set as a nonzero constant. Here, the value of the base b is set as 2.6, and the value of the smooth factor β is set as 0.015. The aforementioned simulated wellbore pressure corresponding to the unit production rate in Fig. 4 can be used to verify the accuracy of the deconvolution results.

Fig. 5 and Fig. 6 show the type-curve comparison of the deconvolution results regarding the wellbore pressure drop and its derivative with the simulation results; they correspond to the Powell's Dog Leg method and the Levenberg-Marquardt method, respectively. From Fig. 7, it is shown that the reconstructed wellbore pressure responses by the deconvolution algorithm corresponding to the two solution methods both have good agreement with the simulated wellbore pressure data corresponding to the variable production rate data, which indicates that the constraint for tuning the deconvolution parameters can be satisfied.

Table 1
Values of reservoir parameters.

Reservoir parameters	Values
Wellbore storage coefficient (bbl/psi)	0.000014
Skin factor	5
Permeability (md)	1
Reservoir thickness (ft)	13.5
Initial pressure (MPa)	30
Porosity	0.1
Well radius (ft)	0.3
Viscosity (cp)	1
Formation volume factor (B/STB)	1
Total compressibility (psi^{-1})	3.0×10^{-6}
Elastic storage ratio of fracture	0.1
Inter-porosity flow coefficient	1.0×10^{-6}

Table 2
The production rate data.

Production duration (Day)	Production rate (STB/D)
1	1.0
4	2.0
5	1.5
10	2.5
30	4.5
50	2.0
100	3.0
200	2.0

However, from Fig. 5, it can be seen that the deconvolved pressure derivative data corresponding to the Levenberg-Marquardt method largely deviate from the one corresponding to the simulation results (Liu et al., 2017), and data divergence also exists especially in the middle of the type curves. Whereas, the deconvolved data of the pressure and the pressure derivative corresponding to the Powell's Dog Leg method have very good agreement with the ones corresponding to the simulation results; and the solution by the method exhibits great convergence ability and numerical stability. Here, the square roots of the sum of the squared residuals at convergence for the overdetermined nonlinear system i.e. Eqs. (10–12) in the Section 2.3, which have been solved by the Powell's Dog Leg method and the Levenberg-Marquardt method respectively, are compared. They are shown in Fig. 8. From Fig. 8, it can be seen that the square roots of the sum of the squared residuals for solving the nonlinear least square problem by the Powell's Dog Leg method and the Levenberg-Marquardt method both decrease with the increase of the number of iterations. However, the square root corresponding to the Powell's Dog Leg method decreases more sharply, and can arrive at a stable smaller value with less iteration times. And the Levenberg-Marquardt method could not decrease the overall error as much as the Powell's Dog Leg method.

Therefore, it can be concluded that the deconvolved pressure derivative for the type curves is very sensitive to the solution methods for the formulated nonlinear least-squares problem. Here, the Powell's Dog Leg method is selected for solving the nonlinear least-squares problem for the stability-improved deconvolution algorithm based on B-splines due to its great performance.

3.2. Analysis of the effects of the base b and the smooth factor β

Different value assignment of the B-spline base b and the smooth factor β may lead to different type curves of the deconvolution results regarding the wellbore pressure drop and its derivative during the nonlinear regularization process. Based on the above simulated case, the effects of the base b and the smooth factor β on the type curves of the deconvolution results are analyzed, respectively. It has been known in the Section 3.1 that the accurate deconvolution results are obtained when the value of b is set as 2.6, and the value of β is set as 0.015.

3.2.1. The effect of the B-spline base b

In order to make sure 2-6 B-spline knots per log cycle, as suggested by Ilk et al. the value of the base b should be on the order of 1.5–3.2 (Liu et al., 2017). Here, the value of the base b is set as 1.5, 1.8, 2.1, 2.4, 2.6, 2.9 and 3.2, respectively. The corresponding type curves of the deconvolution results regarding the wellbore pressure drop and its derivative and the corresponding satisfaction degrees for the constraint conditions are shown in Fig. 9 and Fig. 10, respectively.

From Fig. 9, it can be seen that the values of the base b at the range of 1.5–3.2 have little effect on the type curves of the deconvolution results; just when b is set as 1.5, the curves with red points have little deviation at the initial wellbore storage period. Moreover, from Fig. 10, it can also be seen that the constraint conditions are all satisfied very well. In conclusion, the B-spline base b has little effect on the corresponding (good) satisfaction degree of the constraint conditions i.e. the overall error for

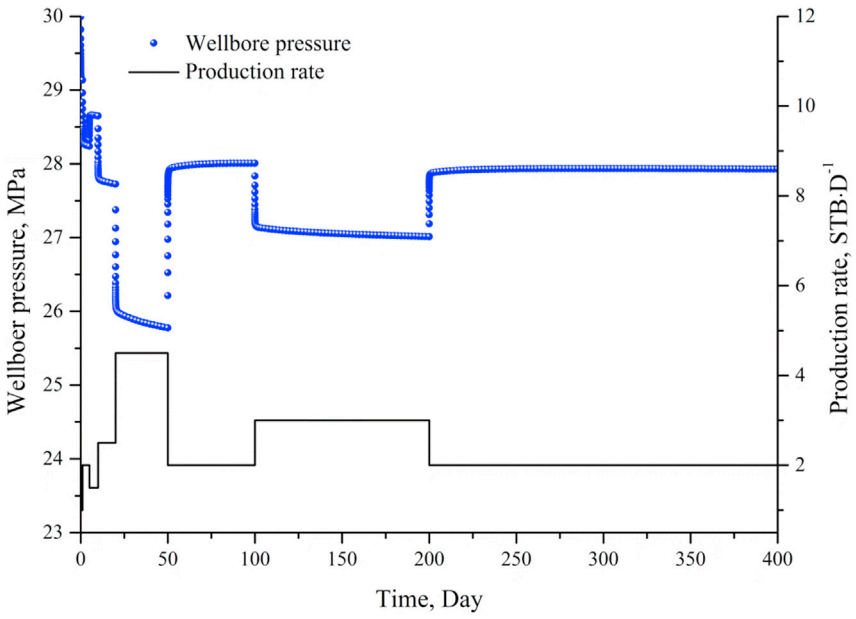

Fig. 3. Wellbore pressure response corresponding to the variable production rate.

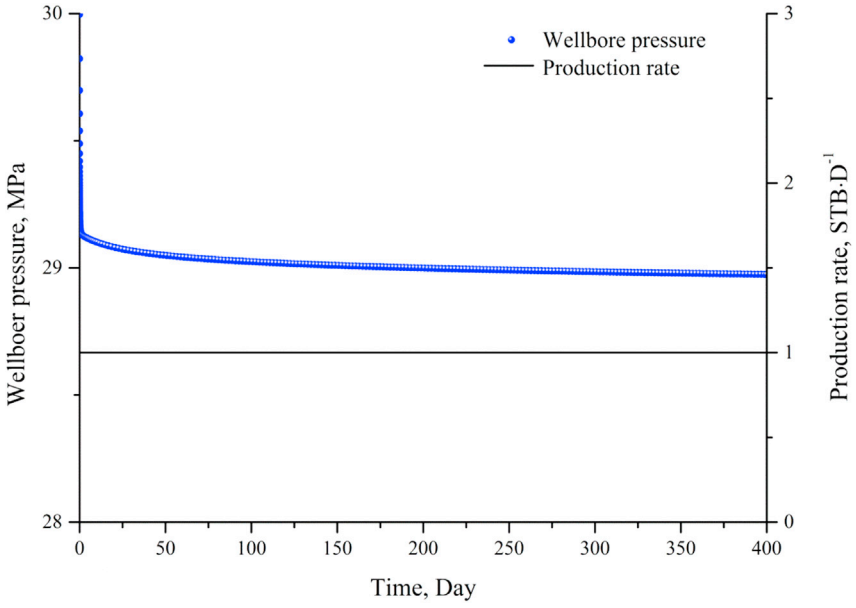

Fig. 4. Wellbore pressure response corresponding to the constant unit production rate.

the solution of the involved nonlinear least square problem. In addition to tuning the value of the smooth factor β, tuning the value of the B-spline base b is another available choice without considering the constraint problems to further improve the stability of the deconvolution algorithm.

3.2.2. *The effect of the smooth factor β*

The smooth factor β represents the magnitude of the nonlinear regularization. Its range is from 0 to 1.0. Here, the value of the smooth factor β is set as 0, 0.005, 0.015, 0.03, 0.06, 0.08, 0.1 and 0.2, respectively. The corresponding type curves of the deconvolution results regarding the wellbore pressure drop and its derivative and the corresponding satisfaction degrees for the constraint conditions are shown in Fig. 11 and Fig. 12, respectively.

From Fig. 11, it can be seen that when the value of the smooth factor β is small, which represents weak nonlinear regularization, data divergence may occur such as the red data points at the initial period when $\beta = 0$; as the smooth factor β increases, data divergence disappears as a result of the nonlinear regularization; and the constraint conditions are all satisfied well when the value of the smooth factor β is set not more than 0.015. It has to be pointed out that due to the reason that small numerical errors may exist in the simulated results, performing the nonlinear regularization is still necessary.

However, from Fig. 11 it can also be seen that as the value of the smooth factor β is up to 0.03, the deconvolved pressure derivative data obviously derivate from the simulated data corresponding to the unit production rate, and the "concave" at the pressure derivative type curves, which directly reflects the type-curve characteristics of the inter-porosity flow between matrix and fractures in the dual-porosity reservoirs, gradually disappears; in one word, type curves of the deconvolution results are distorted. Simultaneously, it can be seen from Fig. 12 that when the value of the smooth factor β is up to 0.03, the reconstructed wellbore pressure response obviously deviates from the simulated wellbore pressure data, and the constraint condition is not satisfied sufficiently; and the larger the value of the smooth factor β, the bigger the deviation.

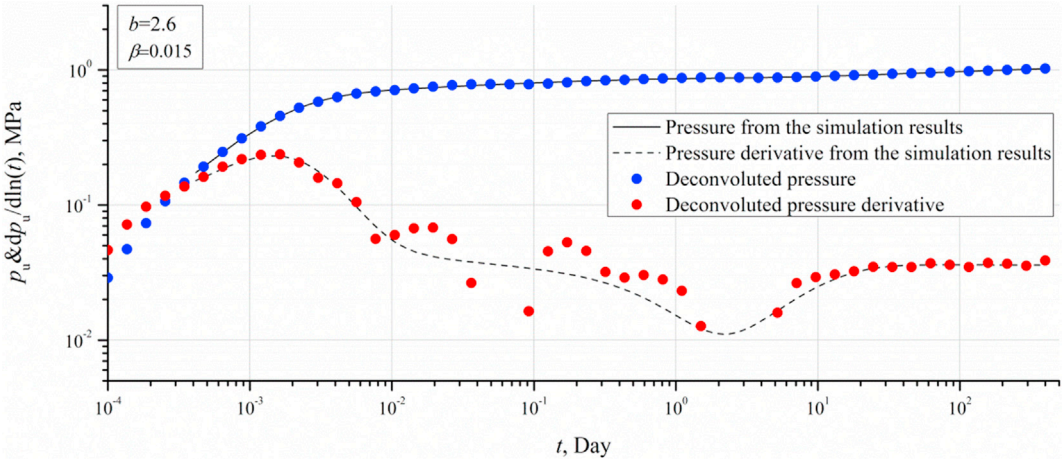

Fig. 5. Type-curve comparison of the deconvolution results by the Levenberg-Marquardt method with the simulation results.

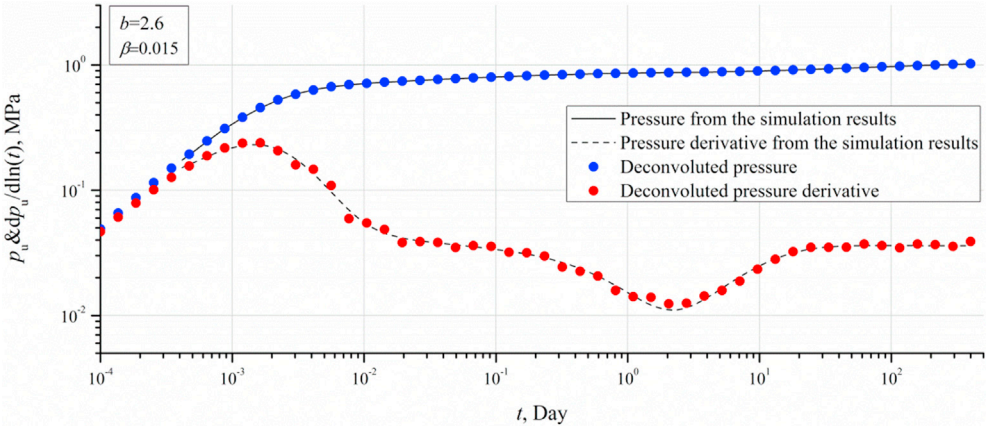

Fig. 6. Type-curve comparison of the deconvolution results by the Powell's Dog Leg method with the simulation results.

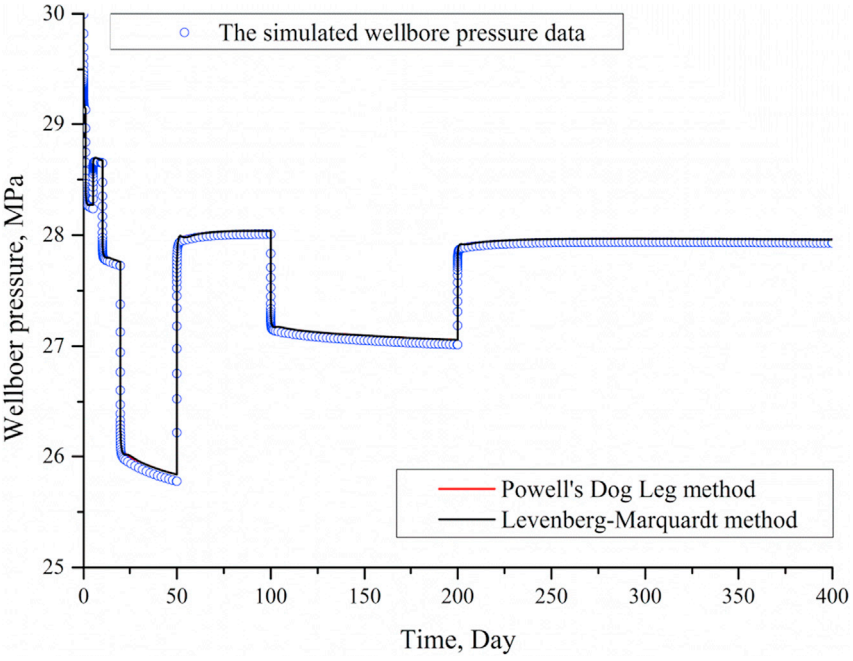

Fig. 7. Comparison of the reconstructed wellbore pressure response with the simulated wellbore pressure data.

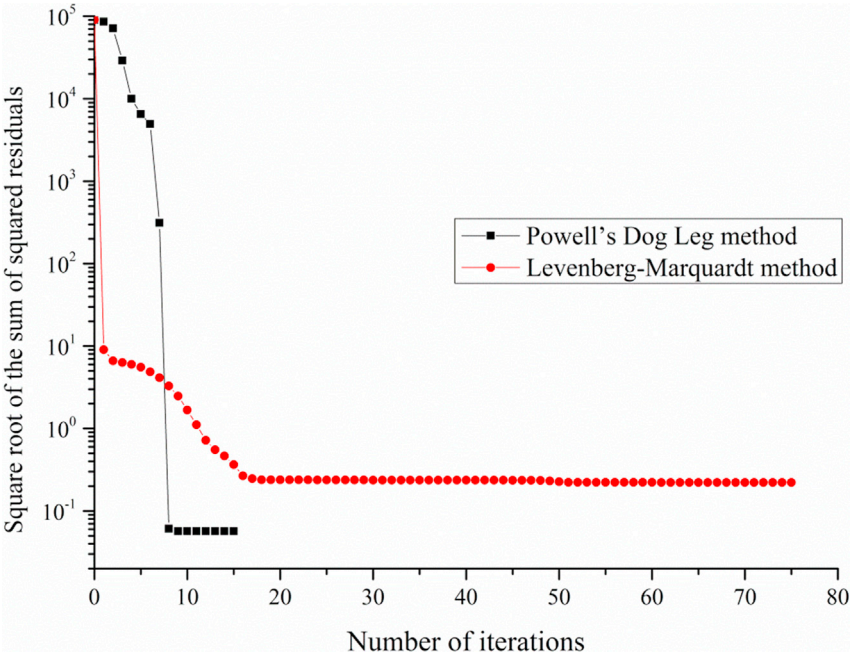

Fig. 8. Comparison of the square roots of the sum of the squared residuals for the overdetermined nonlinear system.

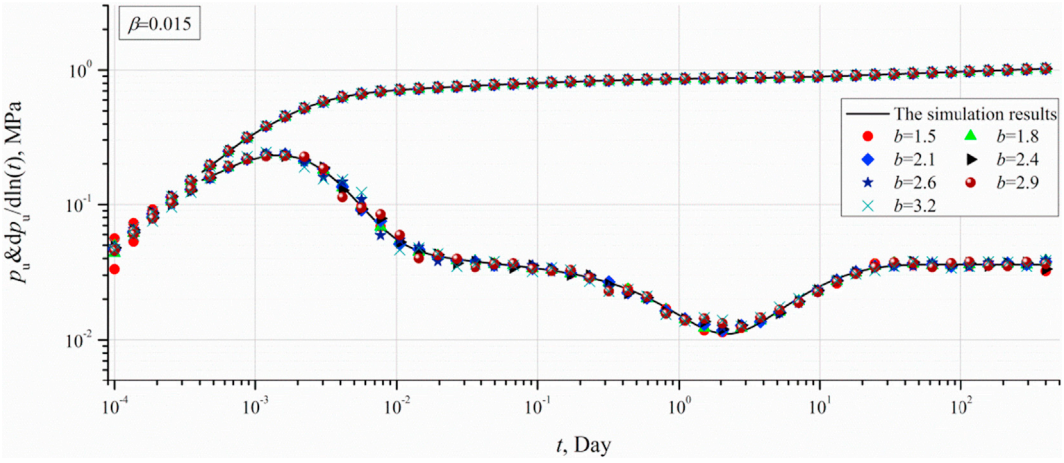

Fig. 9. The effect of the B-spline base b on the type curves of the deconvolution results.

Therefore, it can be concluded that in order to guarantee the correct type curves of the deconvolution results, the constraint conditions should be satisfied as well as possible. In order to make a tradeoff between the smoothness of the pressure derivative type curves and the accuracy of the type-curve characteristics, the optimum value of the smooth factor β should be set as the largest meanwhile the constraint conditions are satisfied.

3.3. Analysis of the effect of the error in the initial formation pressure

Based on the simulated case in the Section 3.1, the effect of the error in the initial formation pressure on the type curves of the deconvolution results is analyzed. From Table 1, it is known that the true initial formation pressure is 30 MPa. Here, the error of the input initial pressure for the deconvolution is set as 1 psi lower than the true initial pressure, 5 psi lower than the true initial pressure, 1 psi higher than the true initial pressure and 5 psi higher than the true initial pressure, respectively (Ahmadi et al., 2017). The corresponding type curves of the deconvolution results regarding the wellbore pressure drop and its derivative and the corresponding satisfaction degrees for the constraint conditions are shown in Fig. 13 and Fig. 14, respectively.

From Figs. 13 and 14, it can be seen that the error of the initial formation pressure mainly affects the late-time wellbore pressure derivative, and some distortion is produced, although the constraint conditions are all satisfied basically. The observations are similar to the ones stated by Onur and Kuchuk (2012). This distortion may lead to incorrect reservoir model identification, particularly the misinterpretation of the reservoir boundaries (Onur and Kuchuk, 2012). Therefore, the initial formation pressure should be estimated accurately for performing the deconvolution algorithm. When the knowledge of initial formation pressure is not accurate enough, fortunately a simple technique has been presented by Levitan et al. (2006) for determining the appropriate value of the initial formation pressure from the well test data; it is based on a trial-and-error procedure by using the deconvolution analysis if the well test data includes several pressure build up periods. This technique is commonly applicable for the deconvolution algorithm presented in this work. Please refer to the reference (Levitan et al., 2006) for the details.

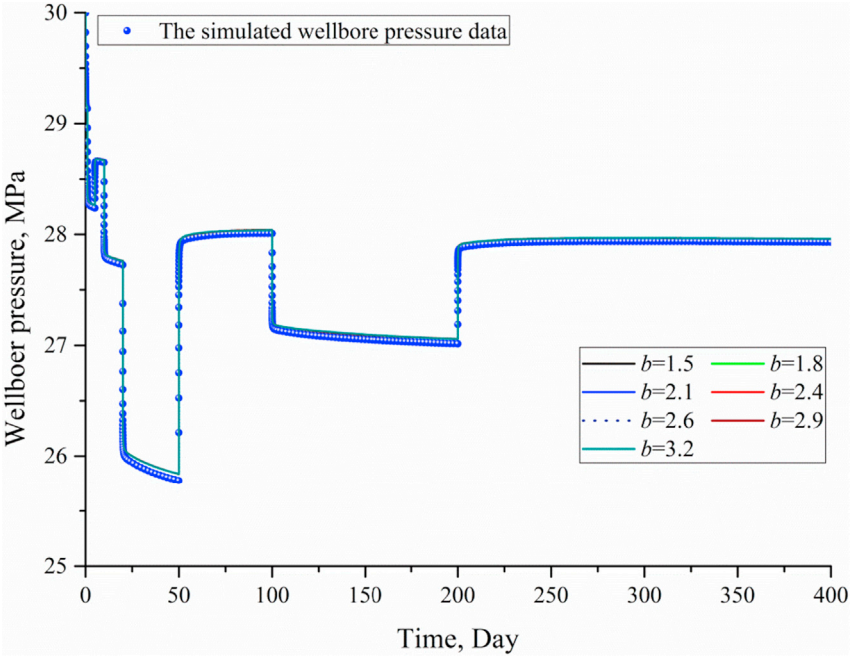

Fig. 10. Comparison of the reconstructed wellbore pressure response corresponding to different values of the B-spline base b with the simulated wellbore pressure data.

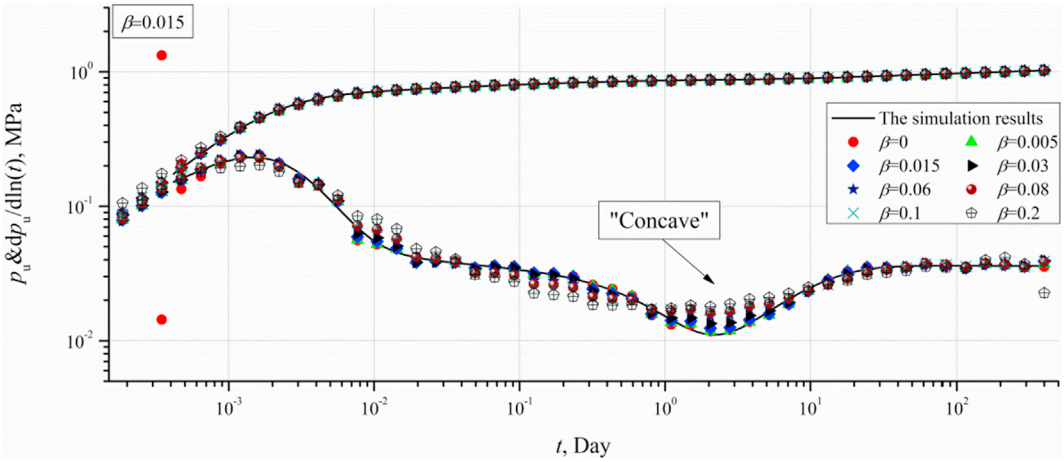

Fig. 11. The effect of the smooth factor β on the type curves of the deconvolution results.

3.4. Statement on how to perform the nonlinear regularization

From the aforementioned analysis, it has been known that determination of the values of the base b and the smooth factor β is very important during the nonlinear regularization process, and different value assignment may lead to different type curves of the deconvolution results regarding the wellbore pressure derivative; it can introduce the uncertainty problem for the subsequent well testing interpretation by the type curve analysis method (Spivey and Lee, 2013). Therefore, it is very significant to state how to perform the nonlinear regularization in order to guarantee the correct type curves of the deconvolution results regarding the wellbore pressure derivative. According to the analysis results on the effects of the base b and the smooth factor β, and also in combination with the actual engineering situations, some principles are presented for the nonlinear regularization process, as follows:

a The value of the base b should be set on the order of 1.5–3.2. In addition to tuning the value of the smooth factor β, tuning the value of the B-spline base b is another available choice to further improve the stability of the deconvolution algorithm without considering the constraint problems.

b The range of the value of the smooth factor β is from 0 to 1.0. The optimum value of the smooth factor β should be set as the largest meanwhile the constraint conditions are satisfied (see Fig. 7 as an example).

c As Liu et al. have suggested in the linear regularization (Liu et al., 2017), it is very necessary to make full use of the accurate knowledge of initial pressure, the knowledge from the sources of reservoir geology and reservoir characterization and other engineering experiences; please refer to the reference (Liu et al., 2017) for the details. Here, this suggestion is also applicable for the nonlinear regularization process; this knowledge can also support useful information for the optimal selection of the values of the base b and the smooth factor β during the nonlinear regularization process. For example, if it is known from the knowledge of reservoir geology that the reservoir is dual-porosity, the type curves of the deconvolution results regarding the wellbore pressure derivative should have the “concave” feature, which represents the inter-porosity flow behavior between matrix

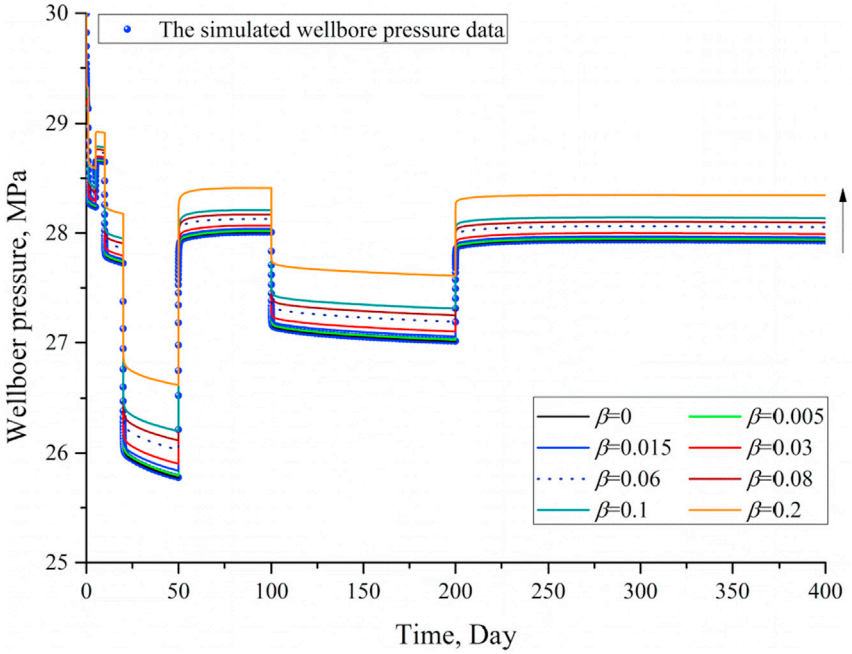

Fig. 12. Comparison of the reconstructed wellbore pressure response corresponding to different values of the smooth factor β with the simulated wellbore pressure data.

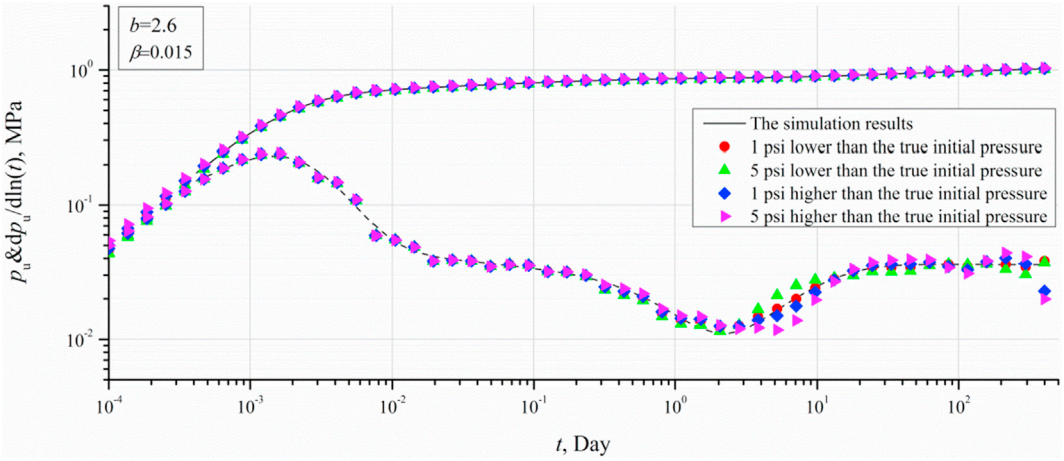

Fig. 13. The effect of the error in the initial formation pressure on the type curves of the deconvolution results.

and fractures in the dual-porosity reservoirs (Liu et al., 2017); and if a pressure build up testing is also conducted at a shut-in period in advance, its accurate type curve regarding the wellbore pressure derivative can provide a direct guidance for the recognition of the type curve of the deconvolution results regarding the wellbore pressure derivative that will be deconvolved at the whole test-time range; after all, the type curves from both the data of the pressure build up testing and the data of the deconvolved wellbore pressure derivative should belong to the same type for the reservoir model identification, but with different time range (Liu et al., 2017).

3.5. Validation of the stability improvement by the nonlinear regularization

3.5.1. The first case study

In order to test the stability improvement by appending the nonlinear regularization, random data errors are added into both the wellbore pressure data and the production rate data of the simulated case (see Fig. 3) in the Section 3.1. 2% random relative error is added into the production rate data, and the data is listed in Table 3; 5% random relative error is added into the wellbore pressure drop corresponding to the variable production rate data; the wellbore pressure data and the production rate data with added data errors are shown in Fig. 15.

Then the deconvolution of the data in Fig. 15 is done by the stability-improved deconvolution algorithm based on B-splines; due to the existence of data errors, the nonlinear regularization has to be performed: the value of b is set as 3.2, and the value of β is set as 0.014. The type curves of the deconvolution results by this algorithm are shown in Fig. 16. Fig. 17 indicates that the corresponding constraint conditions are satisfied very well for the nonlinear regularization. In addition, in order to compare the stability of the aforementioned different deconvolution algorithms, the deconvolution of the data in Fig. 15 is also done by the deconvolution algorithm based on B-splines with the linear regularization (Liu et al., 2017) and by von Schroeter et al.'s deconvolution algorithm (von Schroeter et al., 2002; von Schroeter et al., 2004), respectively; the type curves of their deconvolution results are also shown in Fig. 16. The von Schroeter et al.'s deconvolution algorithm is performed through the KAPPA software, and the default values for the relevant parameters are used; it is worth to mention that the same constraint as shown in Fig. 17 for the stability-improved algorithm by the nonlinear regularization is also satisfied for von Schroeter et al.'s

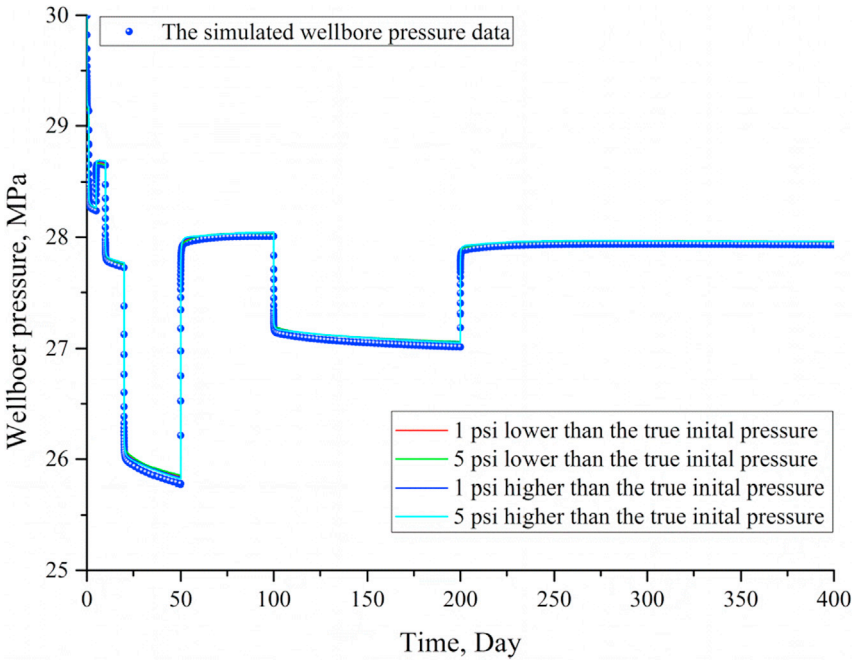

Fig. 14. Comparison of the reconstructed wellbore pressure response corresponding to different errors in the initial formation pressure with the simulated wellbore pressure data.

Table 3
The production rate data with random errors.

Production duration (Day)	Production rate (STB/D)
1	1.0087
4	2.0340
5	1.5153
10	2.5004
30	4.5507
50	2.0375
100	3.0227
200	2.0189

deconvolution algorithm, which can be shown in the KAPPA software.

From Fig. 16, it can be seen that the type curves corresponding to stability-improved deconvolution algorithm based on B-splines by the nonlinear regularization have good agreement with the type curves of the simulation results corresponding to the unit production rate for the whole production duration, and the effect of data errors is mitigated considerably. However, the type curves regarding the pressure derivative corresponding to the deconvolution algorithm based on B-splines with the linear regularization (Liu et al., 2017) and the von Schroeter et al.'s deconvolution algorithm have bad agreement with the type curves of the simulation results. Especially, the type curve regarding the pressure derivative corresponding to the von Schroeter et al.'s deconvolution algorithm has very large deviations, and the shape of the type curve is almost changed; the deconvolution algorithm shows less tolerance to the data errors in the case.

3.5.2. *The second case study*

Here, the stability improvement of the algorithm based on B-splines by appending the nonlinear regularization is also tested through another

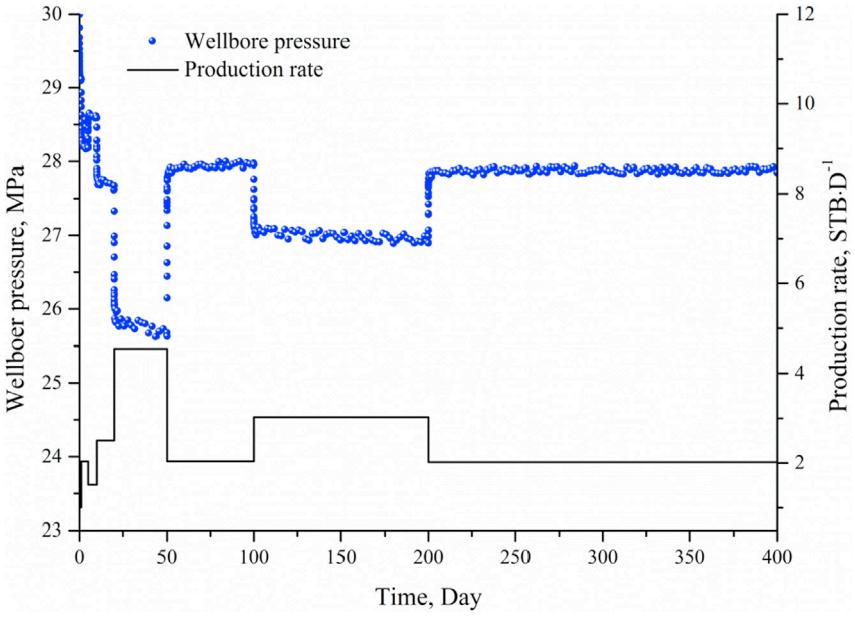

Fig. 15. The wellbore pressure data and the production rate data with random errors.

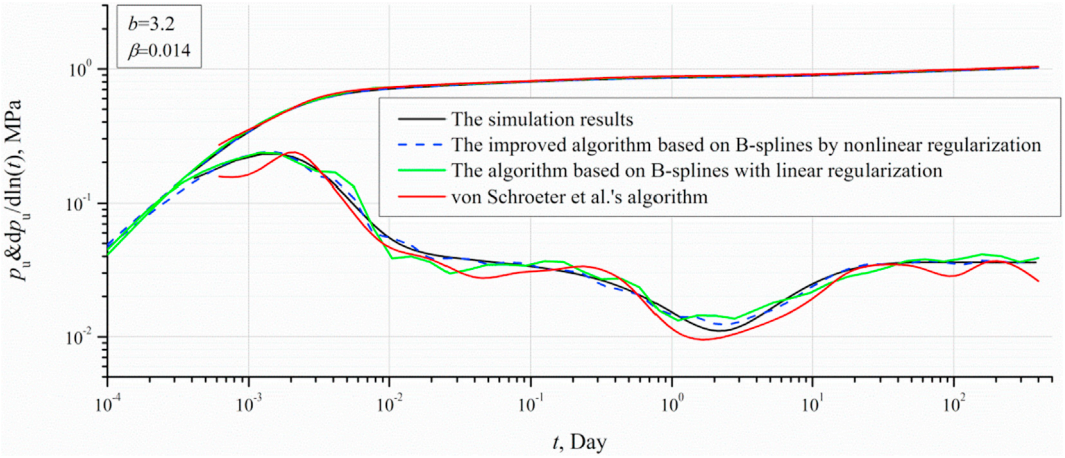

Fig. 16. Type-curve comparison of the deconvolution results by three different algorithms with the simulation results.

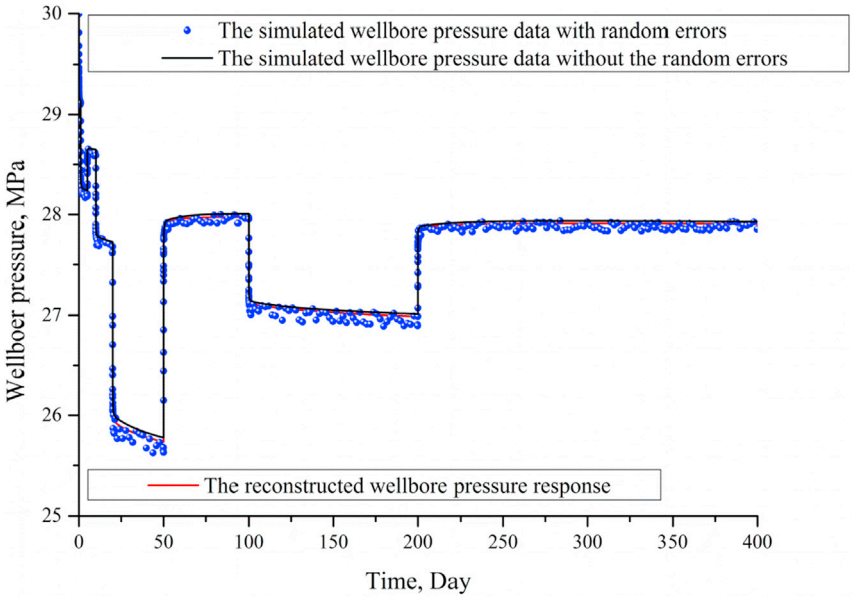

Fig. 17. Comparison of the reconstructed wellbore pressure response with the simulated wellbore pressure data.

simulated case of a vertical well in an infinite dual-porosity reservoir in the reference (Liu et al., 2017); in the case, just 5% random relative error is added in the wellbore pressure drop (Liu et al., 2017); for the nonlinear regularization, the value of b is set as 1.85, and the value of β is set as 0.03; and the constraint conditions are satisfied. As the comparison, the deconvolution is also done by the deconvolution algorithm based on B-splines with the linear regularization and by von Schroeter et al.'s deconvolution algorithm, respectively; the type curves of their deconvolution results are also shown in Fig. 18.

From Fig. 18, it can be clearly seen that the type curves corresponding to the deconvolution algorithm based on B-splines by the nonlinear regularization have the best agreement with the type curves of the simulation results corresponding to the unit production rate for the whole production duration (Liu et al., 2017). However, the type curve regarding the pressure derivative corresponding to the deconvolution algorithm based on B-splines with the linear regularization shows large deviation at the "concave" that can reflect the inter-porosity flow in the dual-porosity reservoirs; and the type curve corresponding to von Schroeter et al.'s deconvolution algorithm also shows obvious deviation at the radial flow period (Spivey and Lee, 2013). Table 4 and Table 5 also show that the comparison of the reservoir parameters obtained from the pressure transient analysis for the three different deconvolution results by three different algorithms for the two case studies in the Section 3.5, as shown in Figs. 16 and 18, with the simulation input data, respectively. From Tables 4 and 5, it can be seen that the reservoir parameters obtained from the pressure transient analysis for the deconvolution results corresponding to the algorithm based on B-splines by appending the nonlinear regularization are the closest to the simulation input data, and then the effect of data errors is largely mitigated; however, some reservoir parameters obtained from the pressure transient analysis corresponding to the algorithm based on B-splines with the linear regularization and von Schroeter et al.'s algorithm have relatively big deviation from the simulation input data, and the effect of data errors is not well mitigated.

Through the study on the two simulated cases with random data errors in the wellbore pressure and production rate data, it can be concluded that when the nonlinear regularization is appended instead of the linear regularization, the stability can be largely improved for mitigating the effect of data errors. What's more, under the same nonlinear regularization method, the representation by B-spline functions in the stability-improved algorithm can exhibit much higher numerical stability than the representation by piecewise linear approximations in von Schroeter et al.'s algorithm (von Schroeter et al., 2002; von Schroeter et al., 2004); it can be attributed to the superior properties of the

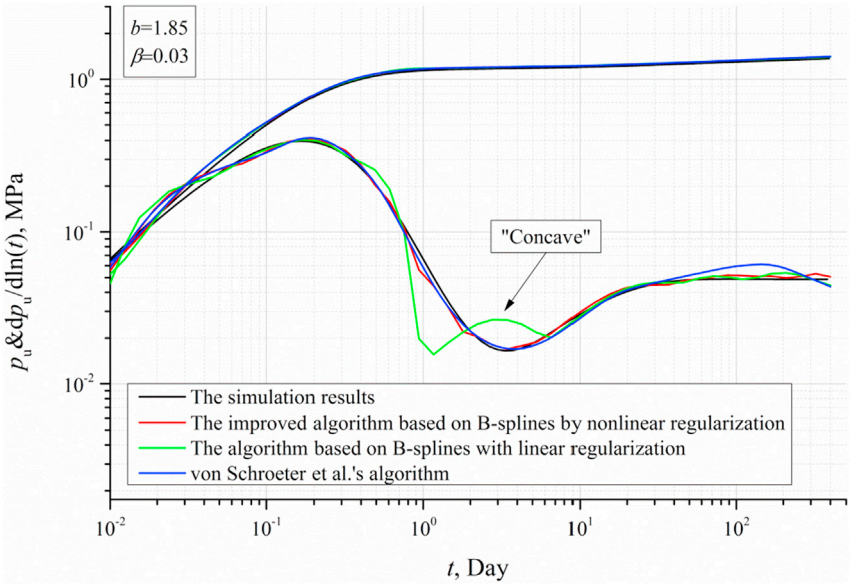

Fig. 18. Type-curve comparison of the deconvolution results by three different algorithms with the simulation results.

Table 4
Comparison of the reservoir parameters obtained from the pressure transient analysis for the three different deconvolution results with the simulation input data for the first case study.

Reservoir parameters	Values			
	Simulation input data	Pressure transient analysis results for the three deconvolution results		
		Algorithms based on B-splines		von Schroeter et al.'s algorithm
		nonlinear regularization	linear regularization	
Initial pressure (MPa)	30	30	30	30
Porosity	0.1	0.1	0.1	0.1
Well radius (ft)	0.3	0.3	0.3	0.3
Viscosity (cp)	1	1	1	1
Formation volume factor (B/STB)	1	1	1	1
Total compressibility (psi^{-1})	3.0×10^{-6}	3.0×10^{-6}	3.0×10^{-6}	3.0×10^{-6}
Elastic storage ratio of fracture	0.1	0.094	0.124	0.11
Inter-porosity flow coefficient	1.0×10^{-6}	9.93×10^{-7}	1.02×10^{-6}	9.03×10^{-7}
Wellbore storage coefficient (bbl/psi)	1.4×10^{-5}	1.38×10^{-5}	1.37×10^{-5}	1.31×10^{-5}
Skin factor	5	4.9	5.64	5.21
Multiply Permeability by Reservoir thickness (md·ft)	13.5	13.5	14	13.4

Table 5
Comparison of the reservoir parameters obtained from the pressure transient analysis for the three different deconvolution results with the simulation input data for the second case study.

Reservoir parameters	Values			
	Simulation input data	Pressure transient analysis results for the three deconvolution results		
		Algorithms based on B-splines		von Schroeter et al.'s algorithm
		nonlinear regularization	linear regularization	
Initial pressure (MPa)	50	50	50	50
Porosity	0.1	0.1	0.1	0.1
Well radius (ft)	0.3	0.3	0.3	0.3
Viscosity (cp)	1.0 cp	1.0	1.0	1.0
Formation volume factor (B/STB)	1.0	1.0	1.0	1.0
Total compressibility (psi^{-1})	3.0×10^{-6}	3.0×10^{-6}	3.0×10^{-6}	3.0×10^{-6}
Elastic storage ratio of fracture	0.1	0.1	0.051	0.065
Inter-porosity flow coefficient	1.0×10^{-6}	1.0×10^{-6}	1.25×10^{-6}	9.17×10^{-7}
Wellbore storage coefficient (bbl/psi)	1.0×10^{-3}	1.0×10^{-3}	9.44×10^{-4}	9.44×10^{-4}
Skin factor	5	5	2.21	3.6
Multiply Permeability by Reservoir thickness (md·ft)	10	9.55	7.47	8.67

representation by B-spline functions in the numerical stability of computations and the built-in smoothness (Jauch et al., 2017).

4. Application to field example

The actual pressure-rate data of the well SapGS02 (Liu et al., 2017) from the example file of KAPPA software is taken for the field example. There are thirteen piecewise production periods with different constant production rates; the last one is the pressure build up period. The measured wellbore pressure data and the measured production rate data for the well SapGS02 are shown in Fig. 19. It is assumed that the basic conditions (Spivey and Lee, 2013) for the application of deconvolution are satisfied for the actual case.

Here, the deconvolution of the actual data is done by the stability-

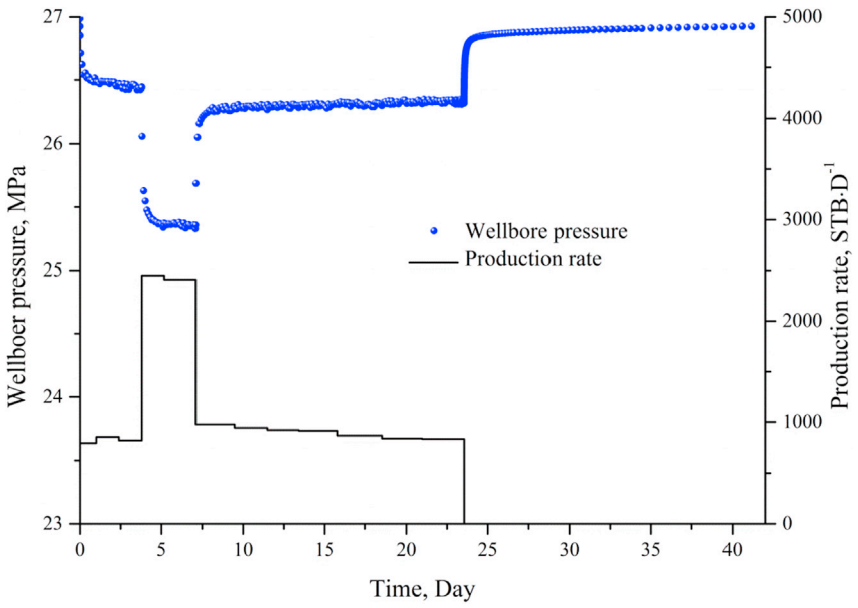

Fig. 19. The measured wellbore pressure data and the measured production rate data for the well SapGS02.

improved deconvolution algorithm based on B-splines by appending the nonlinear regularization. The accurate type curve obtained from the pressure build up period, as shown in the Fig. 13 in the reference (Liu et al., 2017), can provide useful information on the reservoir model identification for identifying the type curves of the deconvolved results during the nonlinear regularization process. Eventually, the value of b is set as 1.7, and the value of β is set as 0.016; the type curves of the deconvolution results by this algorithm are shown in Fig. 20. Fig. 21 indicates that the corresponding constraint conditions are satisfied very well for the nonlinear regularization.

In the reference (Liu et al., 2017), the deconvolution of the actual pressure-rate data has also been done by the deconvolution algorithm based on B-splines with the linear regularization and by von Schroeter et al.'s deconvolution algorithm (by the KAPPA software), respectively; and the type curves of their deconvolution results are also shown in Fig. 20. Then these type curves corresponding to the three different algorithms can be compared in Fig. 20.

From Fig. 20, it can be seen that the type curves, which correspond to the deconvolution algorithm based on B-splines with the linear regularization, oscillates seriously at the initial wellbore storage period; in contrast, the ones, which correspond to the stability-improved deconvolution algorithm based on B-splines by appending the nonlinear regularization, are more stable at this period. The type curves, which correspond to von Schroeter et al.'s deconvolution algorithm, are very smooth; however, due to the strong smoothing treatment in von Schroeter et al.'s deconvolution algorithm, some type-curve characteristics for the reservoir model identification become unnatural, and even distorted, such as the over-smoothed unnatural type curve part at the initial wellbore storage period, the "concave" feature weakening of the type curve regarding the pressure derivative and the turning up of the type curve regarding the pressure derivative at its back end (see Fig. 20). Some of them are just accordant with the analysis results on the effect of the smooth factor β that represents the magnitude of the nonlinear regularization, as discussed at the Section 3.2.

In fact, almost the same smooth degree but distorted type curves with the ones obtained by von Schroeter et al.'s deconvolution algorithm in Fig. 20 can be obtained by the stability-improved deconvolution algorithm based on B-splines through an undue nonlinear regularization (see Fig. 22). For the undue nonlinear regularization, the value of b is set as 2.6, and the value of β is set as 0.9 (a too large value); however, it can be seen from Fig. 23 that the corresponding reconstructed wellbore pressure response has largely deviated from the measured wellbore pressure data,

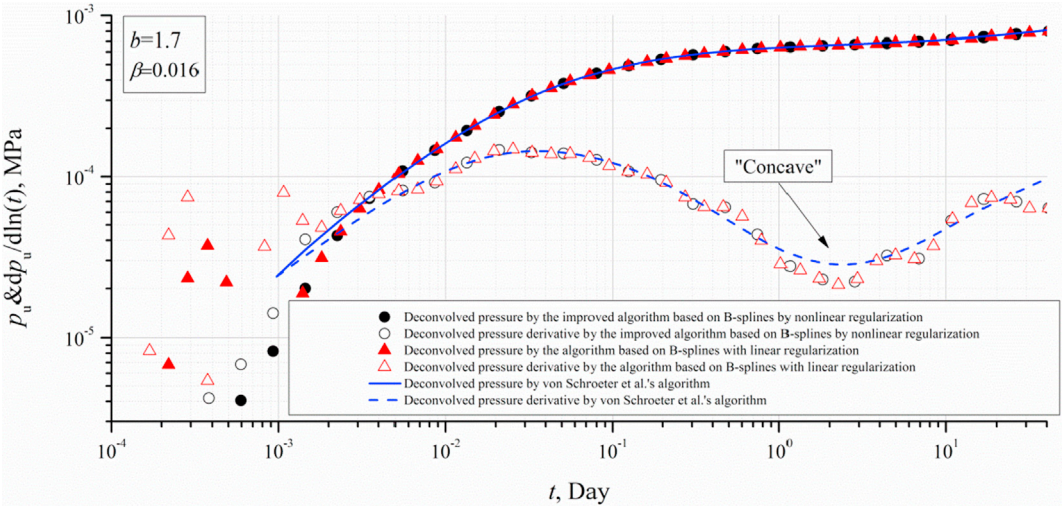

Fig. 20. Type-curve comparison of the deconvolution results by three different algorithms.

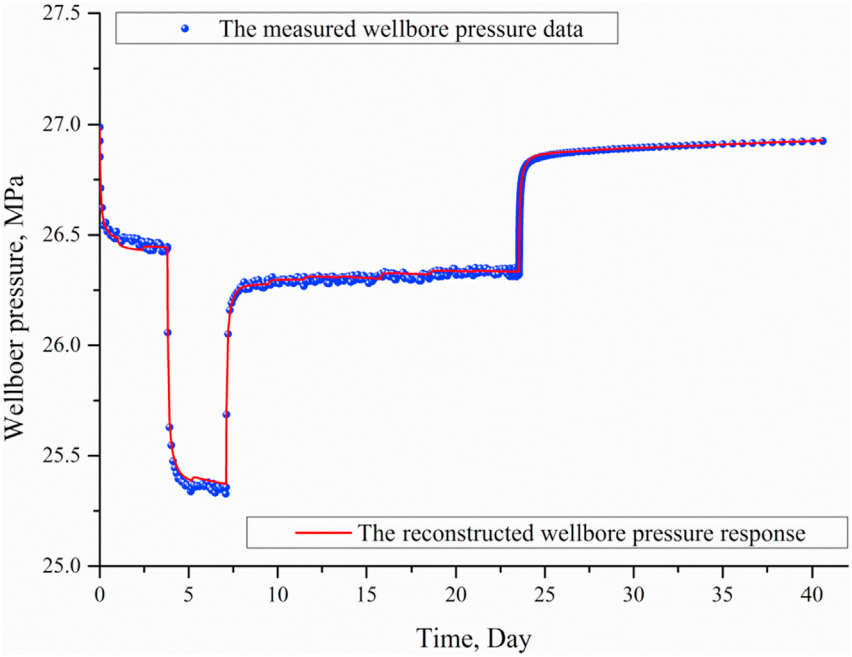

Fig. 21. Comparison of the reconstructed wellbore pressure response with the measured wellbore pressure data.

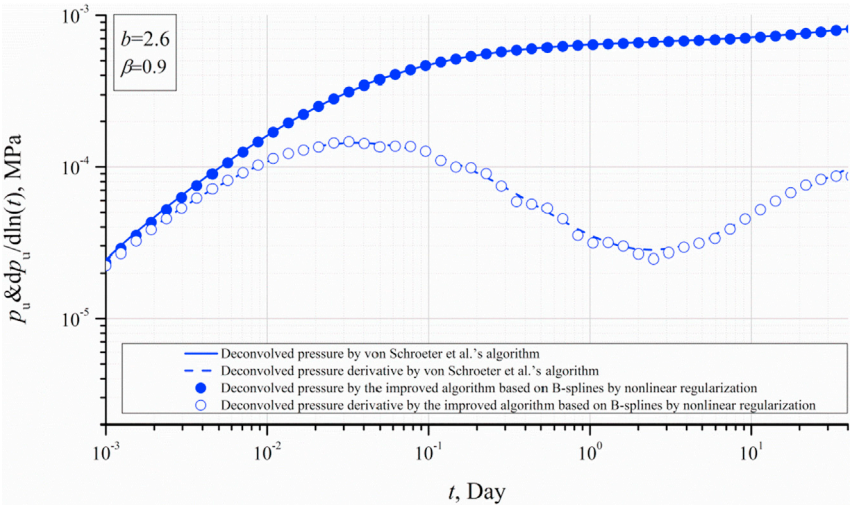

Fig. 22. Type-curve comparison of the two deconvolution results by von Schroeter et al.'s deconvolution algorithm and by the deconvolution algorithm based on B-splines through the undue nonlinear regularization.

and then the constraint conditions for the stability-improved deconvolution algorithm are not satisfied at all; but as for obtaining nearly the same type curves of the deconvolution results (see Fig. 22) by von Schroeter et al.'s deconvolution algorithm, the constraint conditions are still satisfied, which can be shown in the KAPPA software. Therefore, type curve over-smooth problems introduced by the nonlinear regularization may exist in the actual application of von Schroeter et al.'s algorithm. In order to avoid such problems by the undue nonlinear regularization, the corresponding constraint conditions should be satisfied as well as possible for the presented stability-improved deconvolution algorithm.

5. Computational time performance

The comparison of the computation time corresponding to the three different deconvolution algorithms, including the algorithm based on B-splines with the linear regularization, the algorithm based on B-splines with the nonlinear regularization and von Schroeter et al.'s algorithm, for three different simulated cases by the KAPPA software is shown in Table 6. It is necessary to point out that an ordinary computer is used for the deconvolution computation process for every algorithm, which is equipped with double central processing units of 2.10 GHz core frequency and random access memory of 2.00 GB size.

From Table 6, it can be seen that as the number of the pressure data or the number of the rate data increases, the computation time for every deconvolution algorithm increases. Furthermore, the algorithm based on B-splines with the linear regularization has the fastest computation speed mainly due to its analytical solution method for calculating the sensitivity matrix and no numerical iteration workload for the resulted linear least-squares problems (Liu et al., 2017). Although the computation speed decreases due to the numerical iteration workload for the resulted nonlinear least-squares problems when the nonlinear regularization is appended into the stability-improved deconvolution algorithm based on B-splines, its computation speed still stay in the same order with the one of the original algorithm mainly due to the fast analytical solution method for calculating the sensitivity matrix as z-function transformation is not taken. However, the computation time corresponding to the von Schroeter et al.'s algorithm is nearly twenty times more than the one

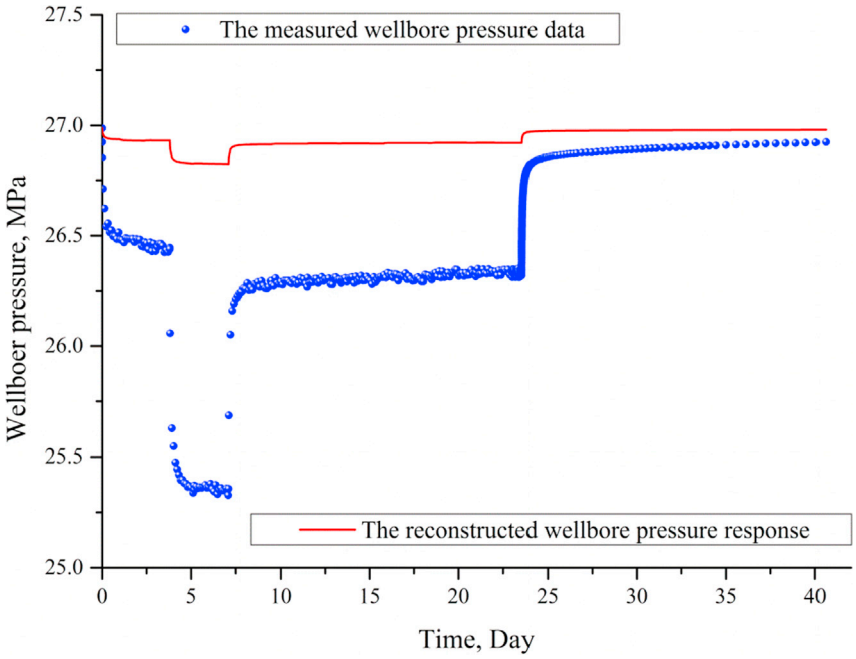

Fig. 23. Comparison of the reconstructed wellbore pressure response with the measured wellbore pressure data.

Table 6
Comparison of the computational time corresponding to three different deconvolution algorithms.

Case name	Number of pressure data	Number of rate data	Computational time, seconds		
			Algorithm based on B-splines with the linear regularization	Algorithm based on B-splines with the nonlinear regularization	von Schroeter et al.'s algorithm
Case A	426	8	0.062	0.187	5.80
Case B	997	8	0.14	0.421	8.46
Case C	1957	16	0.358	0.873	14.78

corresponding to the stability-improved algorithm based on B-splines with the nonlinear regularization, which can be attributed to the more undetermined coefficients and the computational complexity resulted from the z-function transformation in the formulation of von Schroeter et al.'s algorithm (von Schroeter et al., 2002; von Schroeter et al., 2004). It is worth to mention that as the quantity of data largely increases, the stability-improved algorithm based on B-splines with the nonlinear regularization can exhibit the big advantage in the fast computational speed over von Schroeter et al.'s algorithm.

6. Conclusions

1. The previous deconvolution algorithms based on B-splines with the linear regularization have weak stability when data errors exist. In order to improve their stability, a nonlinear regularization method by minimizing the curvature of the deconvolved pressure derivative response, as used in von Schroeter et al.'s algorithm, is appended instead of the linear regularization; and the corresponding nonlinear regularization equations are appropriately deduced. The reformulated nonlinear least-squares problem can be solved stably by the advanced Powell's Dog Leg method.
2. In comparison with von Schroeter et al.'s algorithm, the transformation of the convolution equation i. e. Eq. (1) by the nonlinear z function is avoided in the stability-improved algorithm based on B-splines with the nonlinear regularization; the whole deconvolution process can be simplified; and the sensitivity matrix of the basic linear system from the measured pressure and rate data can be solved directly by the piecewise analytical integration method, which can largely improve the deconvolution computation speed. Moreover, it has been demonstrated through all the case study in the paper that the deconvolved $dp_u/d\ln(t)$ by the stability-improved algorithm can still keep positive for the plotting of type curves although the z-function transformation is avoided.
3. As a whole, the presented stability-improved algorithm in the paper can inherit good "genes" from their "parents" i. e. the improved version of Ilk et al.'s algorithm based on B-splines with the linear regularization and von Schroeter et al.'s algorithm. These good "genes" include the representation of p'_u by B-splines, no complicated z-function transformation of the convolution equation, the fast analytical solution method for calculating the elements of the sensitivity matrix and the nonlinear regularization method.
4. A constraint condition for tuning the values of the B-spline base b and the smooth factor β is presented for restricting the nonlinear regularization process. The effects of the base b and the smooth factor β on the type curves of the deconvolution results are analyzed. And the effect of the error in the initial formation pressure on the type curves of the deconvolution results is also analyzed. Then a statement on how to perform the nonlinear regularization is presented specifically.
5. Through the simulated case study and the actual case study, it is concluded that the stability-improved algorithm based on B-splines by the nonlinear regularization exhibits much better stability when data errors exist than both the original algorithm based on B-splines with the linear regularization and von Schroeter et al.'s algorithm; the over smooth problem of the type curves regarding the deconvolved pressure derivative by the undue nonlinear regularization may exist in the actual application of von Schroeter et al.'s algorithm. In order to avoid the over smooth problem by the undue nonlinear regularization, the corresponding constraint conditions should be satisfied as well as possible for the presented stability-improved deconvolution algorithm.
6. Through the simulated case test, it is also concluded that the stability-improved algorithm based on B-splines by the nonlinear regularization has the same high level computation speed with the original algorithm based on B-splines with the linear regularization; and the

computation speed of the stability-improved algorithm based on B-splines is nearly twenty times more than that of von Schroeter et al.'s algorithm.

Acknowledgement

The authors would like to acknowledge the fundings by the project (Grant No. 51404232) sponsored by the Natural Science Foundation of China (NSFC), the National Science and Technology Major Projects (Grant No. 2011ZX05038003; Grant No. 2011ZX05046-03) and the project (Grant No. 2014M561074) by the China Postdoctoral Science Foundation.

References

Ahmadi, M., Sartipizadeh, H., Ozkan, E., 2017. A new pressure-rate deconvolution algorithm based on Laplace transformation and its application to measured well responses. J. Petrol. Sci. Eng. 157, 68–80.

Al-Ajmi, N., Ahmadi, M., Ozkan, E., Kazemi, H., 2008. Numerical inversion of Laplace transforms in the solution of transient flow problems with discontinuities. In: SPE 116255 Presented at the 2008 SPE Annual Technical Conference and Exhibition. Denver, Colorado, USA, 21–24 September.

Çınar, M., IlK, D., Onur, M., Valkó, P.P., Blasingame, T.A., 2006. A comparative study of recent robust deconvolution algorithms for well-test and production-data analysis. In: SPE 102575 Presented at the 2006 SPE Annual Technical Conference and Exhibition. San Antonio, Texas, USA, 24–27 September.

IlK, D., 2005. Deconvolution of Variable Rate Reservoir Performance Data Using B-splines. Texas A&M University, College Station, Texas. December 2005.

IlK, D., Valkó, P.P., Blasingame, T.A., 2005. Deconvolution of variable-rate reservoir-performance data using B-splines. In: SPE 95571 Presented at the 2005 SPE Annual Technical Conference and Exhibition. Dallas, Texas, USA, 9–12 October.

Jauch, J., Bleimund, F., Rhode, S., Gauterin, F., 2017. Recursive B-spline approximation using the Kalman filter. Eng. Sci. Technol. Int. J. 20, 28–34.

Liu, W.C., Liu, Y.W., Han, G.F., Zhang, J.Y., Wan, Y.Z., 2017. An improved deconvolution algorithm using B-splines for well-test data analysis in petroleum engineering. J. Petrol. Sci. Eng. 149, 306–314.

Levitan, M.M., 2005. Practical application of pressure/rate deconvolution to analysis of real well tests. SPE Reservoir Eval. Eng. 8 (2), 113–121.

Levitan, M.M., Crawford, G.E., Hardwick, A., 2006. Practical considerations for pressure-rate deconvolution of well-test data. SPE J. 11 (1), 35–47.

Madsen, K., Nielsen, H.B., Tingleff, O., 2004. Methods for Non-linear Least Squares Problems, 2th ed. Informatics and Mathematical Modelling, Technical University of Denmark.

Onur, M., Çinar, M., Ilk, D., Valko, P.P., Blasingame, T.A., Hegeman, P.S., 2008. An investigation of recent deconvolution methods for well-test data analysis. SPE J. 13 (2), 226–247.

Onur, M., Kuchuk, F.J., 2012. A new deconvolution technique based on pressure-derivative data for pressure-transient-test interpretation. SPE J. 17 (1), 307–320.

Shterenlikht, A., Alexander, N.A., 2012. Levenberg-Marquardt vs Powell's dogleg method for Gurson-Tvergaard-Needleman plasticity model. Comput. Meth. Appl. Mech. Eng. 237–240, 1–9.

Spivey, J.P., Lee, W.J., 2013. Applied Well Test Interpretation. SPE Textbook Series, Richardson.

von Schroeter, T., Hollaender, F., Gringarten, A.C., 2002. Analysis of well test data from downhole permanent downhole gauges by deconvolution. In: SPE 77688 Presented at the 2002 SPE Annual Technical Conference and Exhibition. San Antonio, Texas, USA, 29 September-2 October.

von Schroeter, T., Hollaender, F., Gringarten, A.C., 2004. Deconvolution of well test data as a nonlinear total least squares problem. SPE J. 9 (4), 375–390.